Proc. Natl. Acad. Sci. USA
Vol. 93, pp. 2629–2634, April 1996
Biochemistry

Barriers to protein folding: Formation of buried polar interactions is a slow step in acquisition of structure

(refolding kinetics/Arc repressor/diffusion limit/transition state/folding intermediate)

CAREY D. WALDBURGER, THORLAKUR JONSSON, AND ROBERT T. SAUER

Department of Biology, Massachusetts Institute of Technology, Cambridge, MA 02139-4307

Communicated by Leonard S. Lerman, Massachusetts Institute of Technology, Cambridge, MA, December 18, 1995 (received for review October 24, 1995)

ABSTRACT **In the MYL mutant of the Arc repressor dimer, sets of partially buried salt-bridge and hydrogen-bond interactions mediated by Arg-31, Glu-36, and Arg-40 in each subunit are replaced by hydrophobic interactions between Met-31, Tyr-36, and Leu-40. The MYL refolding/dimerization reaction differs from that of wild type in being 10- to 1250-fold faster, having an earlier transition state, and depending upon viscosity but not ionic strength. Formation of the wild-type salt bridges in a hydrophobic environment clearly imposes a kinetic barrier to folding, which can be lowered by high salt concentrations. The changes in the position of the transition state and viscosity dependence can be explained if denatured monomers interact to form a partially folded dimeric intermediate, which then continues folding to form the native dimer. The second step is postulated to be rate limiting for wild type. Replacing the salt bridge with hydrophobic interactions lowers this barrier for MYL. This makes the first kinetic barrier rate limiting for MYL refolding and creates a downhill free-energy landscape in which most molecules which reach the intermediate state continue to form native dimers.**

Some protein-folding reactions can be completed on the submillisecond time scale (1, 2), while others require hours or even longer times (3). Why are the kinetic barriers to folding high for one protein and low for another? Is the folding rate determined by the overall structural class or global fold of a protein? Are certain types of structural elements or motifs intrinsically difficult to assemble? At present, there are relatively few experiments which address such questions. In some instances, folding reactions have been shown to be limited by slow processes such as *cis-trans* proline isomerization or disulfide-bond formation (4, 5). However, folding rates can still vary enormously when proline isomerization is not significant and proteins do not contain disulfide bonds. In this paper, we show that a protein-folding reaction can be accelerated significantly by amino acid substitutions which replace a partially buried hydrogen-bond/salt-bridge network in Arc repressor with hydrophobic interactions. This suggests that forming native polar interactions in a relatively hydrophobic environment is an inherently difficult step, which slows folding.

The native form of the Arc repressor of bacteriophage P22 is a dimer in which identical monomers wrap around each other to form a single globular domain (6, 7). Folding and dimerization of Arc appear to be concurrent events, as formation of the dimer from two denatured monomers occurs without detectable intermediates in both equilibrium and kinetic studies (8, 9). The refolding/dimerization reaction is also relatively fast, with a half-time of ≈10 ms at a protein concentration of 10 μM (9). Wild-type Arc contains two salt-bridge triads, formed by the side chains of Arg-31, Glu-36, and Arg-40 in each monomer (refs. 10 and 11; C. Kissinger, U. Obeysekare, L. Keefe, B. Raumann, R.T.S., and C. Pabo, unpublished results). The Glu-36 side chain is inaccessible to solvent and forms charge-stabilized hydrogen bonds with the partially buried Arg-31 and Arg-40 side chains. Combinatorial mutagenesis studies have shown that these salt-bridge triads can be replaced by many different combinations of hydrophobic residues (12). The crystal structure of one such mutant, in which the salt bridge is replaced by Met-31, Tyr-36, and Leu-40 (MYL), reveals that the wild-type hydrogen-bond and salt-bridge interactions are replaced by hydrophobic-packing interactions with almost no change in the overall structure of the mutant protein (12). In fact, the MYL protein is biologically active as a repressor *in vivo*, binds operator DNA tightly and specifically *in vitro*, and is approximately 3.9 kcal/mol of dimer (1 kcal = 4.18 kJ) more stable than the wild-type protein (12).

MATERIALS AND METHODS

Proteins. The MYL mutant used for the studies described here contains the st11 C-terminal extension (-His-His-His-His-His-His-Gln-Asn-Lys-His-Glu). This unstructured tail reduces susceptibility to intracellular proteolysis and allows affinity purification but has no significant effect on the stability or folding kinetics of otherwise wild-type Arc (13). To eliminate any small differential effects of the tail sequence, the refolding properties of MYL-st11 were compared with those of Arc-st11. Both proteins were purified to homogeneity by chromatography on Ni^{2+}-NTA (nitrilotriacetate) agarose (Qiagen, Chatsworth, CA) and SP-Sephadex (Pharmacia) as described previously (12, 14).

Renaturation Kinetics. Refolding experiments were monitored by changes in intrinsic tryptophan fluorescence measured by using an Applied Photophysics DX17.MV stopped-flow instrument. The MYL-st11 and Arc-st11 proteins were unfolded in buffer containing 50 mM Tris·HCl, at pH 7.5, 50 mM KCl, and 4.5–7.5 M urea. Refolding reactions were initiated by rapid dilution to a final urea concentration of 0.5–2.75 M. In most reactions, the final protein concentration was 2 μM. For studies of salt or viscosity dependence, the buffers were supplemented with additional KCl or sucrose as needed. Unless noted, refolding experiments were performed at 25°C.

Under the final conditions used for refolding experiments, the MYL mutant is greater than 95% folded and thus the dissociation rate can effectively be ignored in the refolding rate expression

$$2\frac{d[N_2]}{dt} = -\frac{d[U]}{dt} \approx k_f[U]^2,$$

where k_f is the second-order rate constant for refolding/dimerization and $[N_2]$ and $[U]$ are the concentrations of native dimer and denatured monomer, respectively. Refolding data

The publication costs of this article were defrayed in part by page charge payment. This article must therefore be hereby marked "*advertisement*" in accordance with 18 U.S.C. §1734 solely to indicate this fact.

for the MYL mutant were fit by nonlinear least-squares procedures using the program NONLIN (15, 16) to the equation

$$F = F_0 + F_1\left(1 - \frac{[U]}{[P_t]}\right) = F_0 + F_1\left(\frac{k_{app}\cdot t}{1 + k_{app}\cdot t}\right),$$

where F, F_0, and F_1 are the observed fluorescence, initial fluorescence, and fluorescence amplitude, respectively, k_{app} is $[P_t]\cdot k_f$ (where $[P_t]$ is the total protein concentration in monomer equivalents), and t is time (9). Arc-st11 is less stable than MYL (12, 13) and under some of the refolding conditions used (1–2 M urea, 30–40°C) is less than 90% folded at equilibrium. Under such conditions, the unfolding rate also needs to be considered:

$$-\frac{d[U]}{dt} = k_f[U]^2 - 2k_u[N_2].$$

As a result, wild-type refolding data were fit to equations which include both the association and dissociation reactions (9). In such cases, values of the unfolding rate constant (k_u) were determined by linear extrapolation of log k_u versus urea concentration plots (9).

RESULTS

MYL Refolds Faster than Wild Type. Fig. 1 shows refolding experiments for wild-type Arc and the MYL mutant at a protein concentration of 2 μM, pH 7.5, and 50 mM KCl after rapid dilution from unfolding conditions (4.5 M urea for wild type; 7.5 M urea for MYL) to refolding conditions (1.25 M urea). A single refolding phase accounting for the expected change in amplitude is observed in both cases, but the MYL mutant refolds much faster than wild type. Clearly, formation of the wild-type salt bridges and hydrogen bonds between Arg-31, Glu-36, and Arg-40 in Arc results in a significantly higher kinetic barrier to refolding than formation of the hydrophobic contacts between Met-31, Tyr-36, and Leu-40 in the MYL protein. Fitting of the refolding trajectories to a second-order reaction gives values of k_{app} of approximately 260 s^{-1} for MYL and 1.7 s^{-1} for wild type. The wild-type refolding reaction has been shown to be bimolecular by the criterion that k_{app} values display the expected linear dependence ($k_{app} = [P_t]\cdot k_f$) on protein concentration (9). As shown in Fig. 2, this linear dependence is also observed for refolding of the MYL mutant. Thus, the transition states for refolding of both proteins must be dimeric.

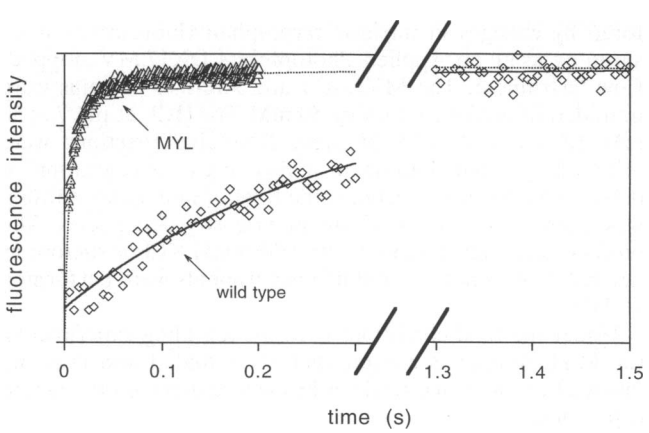

FIG. 1. Refolding kinetics for Arc-st11 and MYL-st11 at 25°C, 1.25 M urea, 50 mM Tris·HCl at pH 7.5, 50 mM KCl, and 2 μM protein. Proteins were unfolded in urea and refolding was initiated by rapid mixing with a 5-fold excess of buffer containing sufficient urea to give a final concentration of 1.25 M. The lines are theoretical bimolecular refolding curves calculated with k_{app} = 260 s^{-1} for MYL and k_{app} = 1.7 s^{-1} for wild type.

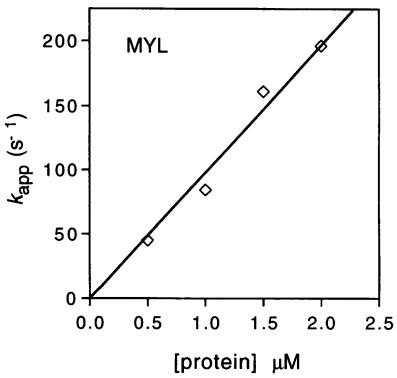

FIG. 2. Linear dependence of MYL refolding rate on protein concentration. Values of k_{app}, calculated from experiments like those shown in Fig. 1, are plotted on the y-axis. Refolding rates were determined at final conditions of 25°C, 1.25 M urea, 50 mM Tris·HCl at pH 7.5, and 50 mM KCl.

Urea Dependence and Transition State Solvation. Refolding experiments for the MYL protein and wild-type Arc were carried out at different final urea concentrations, revealing an approximate linear dependence of log k_f on urea concentration in each case (Fig. 3*A*). Extrapolation of the MYL data to 0 M urea predicts a refolding rate constant of approximately $3\cdot10^8$ $M^{-1}\cdot s^{-1}$. Thus, collisions that lead to productive folding of MYL monomers occur at a rate about 1/3 of the estimated diffusion limit ($\approx10^9$ $M^{-1}\cdot s^{-1}$; ref. 9). The wild-type refolding rate constant calculated by extrapolation is about $8\cdot10^6$ $M^{-1}\cdot s^{-1}$ in the absence of urea. At equivalent protein concentrations, the MYL mutant refolds roughly 40-fold faster than wild type in the absence of urea and 1250-fold faster in 3 M urea (Fig. 3*A*). The urea dependences of the refolding rates are obviously substantially different for the two proteins. The value of k_f for wild-type Arc decreases by 7-fold for every 1 M increase in urea, but the value of k_f for the MYL mutant decreases only by 2.1-fold over each 1 M urea interval.

The decreased urea dependence of the MYL refolding reaction compared with the wild-type reaction suggests that significantly less surface area is buried between denatured MYL and the MYL transition state than between denatured Arc and the wild-type transition state (18, 19). The fractional position of the refolding transition state along a reaction coordinate defined by solvent accessibility can be calculated as m_f/m, where m_f is the slope of a plot of $-RT\ln(k_f)$ vs. urea concentration and m is the slope of a plot of $-RT\ln(K_u)$ vs. urea concentration. For wild-type Arc, $m_f/m \approx 0.75$, indicating that roughly three-quarters of the total surface, which becomes solvent inaccessible during folding, is buried by the time the transition state is reached. For MYL, $m_f/m \approx 0.4$, suggesting that less than half of the surface area, which becomes solvent inaccessible during folding, is buried in the transition state. Thus, the MYL mutations increase the refolding rate and also shift the transition state to a point substantially earlier in the refolding reaction in terms of buried surface area.

Temperature Dependence of Refolding. An Arrhenius plot of the temperature dependence of the wild-type and MYL refolding reactions is shown in Fig. 3*B*. The MYL refolding reaction remains substantially faster than the wild-type reaction over the entire temperature range. The downward curvature of both plots would be expected for a two-state reaction if the heat capacity of the denatured protein were higher than that of the transition state (17). For a multistate reaction, such curvature could also be caused by a change in the rate-limiting step. The MYL refolding reaction reaches a maximum near 30°C, while the wild-type reaction reaches a maximum near

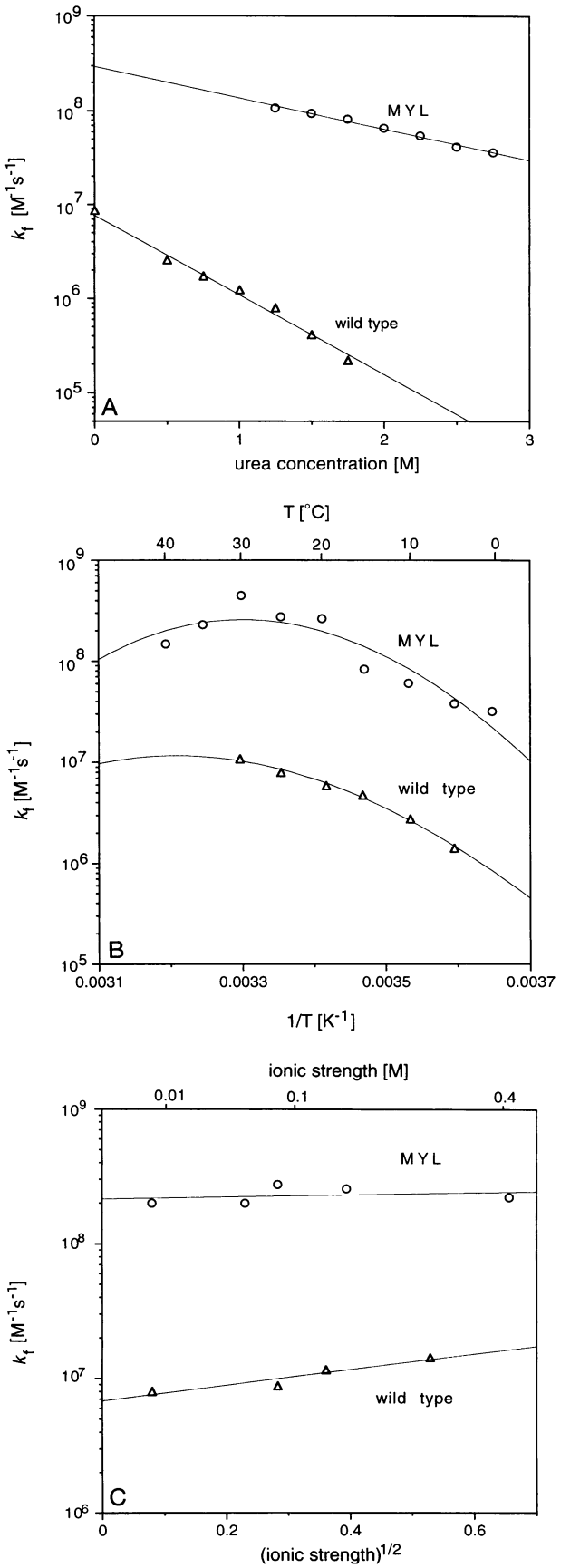

FIG. 3. (*A*) Urea dependence of wild-type and MYL refolding reactions (25°C, 50 mM Tris·HCl at pH 7.5/50 mM KCl/2 μM protein). Values of k_f were calculated as $k_{app}/[P_t]$. For wild type, the experimental point at 0 M urea was determined by a pH-jump experiment (9). (*B*) Arrhenius plot of the temperature dependence of refolding rate constants. k_f values in the absence of urea were determined by extrapolation of $\log(k_f)$ vs. urea concentration plots of refolding data at different temperatures. Experiments were performed in 50 mM Tris·HCl at pH 7.5/50 mM KCl/2 μM protein. The lines are nonlinear least-squares fits to the equation $y = A + B(293/T) + C\ln(293/T)$ (ref. 17) with fitted parameters $A = 339.4$, $B = -323.7$, $C = 304.3$ (wild type) and $A = 508.4$, $B = 489.3$, $C = 473.0$ (MYL). (*C*) Ionic strength dependence of refolding rate constants. k_f values in the absence of urea were determined by extrapolation of $\log(k_f)$ vs. urea concentration plots of refolding data at different KCl concentrations. Experiments were performed at 25°C, in 50 mM Tris·HCl at pH 7.5 and 2 μM protein. The slopes of the linear least-squares fits are 0.59 (wild-type) and 0.081 (MYL).

40°C. This indicates that the activation enthalpies for the refolding reactions are effectively zero at these temperatures. It is important to note, however, that both the MYL and wild-type reactions have substantial activation enthalpies (as much as 20–30 kcal/mol) at lower temperatures.

Salt Dependence of Refolding. As shown in Fig. 3*C*, the refolding rate of MYL is effectively independent of ionic strength, while the refolding rate of wild-type Arc increases with ionic strength (9). Thus, some of the increase in the MYL folding rate relative to wild type appears to result from the elimination of unfavorable electrostatic interactions mediated by the wild-type Arg-31, Glu-36, and/or Arg-40 side chains. Ions in bulk solvent are apparently able to screen these interactions to some extent, but even at high ionic strength the MYL mutant still refolds 10- to 20-fold faster than wild type.

Viscosity Dependence. As the solvent viscosity increases, the MYL refolding rate decreases in a linear fashion with a slope near 1 (Fig. 4). This is consistent with a reaction in which the rate-determining step is diffusion controlled (20). By contrast, the refolding rate of wild-type Arc increases slightly as the viscosity increases (Fig. 4). The absence of significant viscosity dependence for the wild-type refolding/dimerization reaction is difficult to rationalize if the encounter complex for wild-type dimerization represents the highest free-energy state along the reaction coordinate. If, on the other hand, the encounter complex represents a lower energy state, then one needs to explain why the wild-type refolding reaction is concentration dependent (9). As discussed below, these observations can be reconciled in a model which includes a partially folded dimeric intermediate which, for wild-type Arc, rapidly preequilibrates with denatured monomers.

DISCUSSION

The native dimer structures of wild-type Arc and the MYL mutant are extremely similar (≈0.7-Å rms deviation in C^α positions; ref. 12), with differences predominantly in the side-chain interactions mediated by residues 31, 36, and 40 (Fig. 5 *A* and *B*). In wild-type Arc, these side chains are partially buried and form hydrogen bonds and salt bridges with each other. In MYL, the mutant side chains are hydrophobic and pack against each other. Depending on the urea and salt concentration, we observe from a 10-fold to greater than a 1000-fold increase in the rate of refolding of MYL relative to wild type. This difference in refolding rates indicates that formation of the wild-type hydrogen bonds and salt bridges in a relatively hydrophobic environment must be a difficult step in refolding. The effects of alanine-substitution mutations on the refolding and unfolding kinetics of Arc have been interpreted to suggest that most native interactions take place without proper geometry in the transition state (21). By this model, it makes physical sense that establishment of hydrogen-bond and salt-bridge interactions in a partially buried environment would be difficult. Effectively, the energetic penalty for desolvation of the polar atoms would need to be paid in the

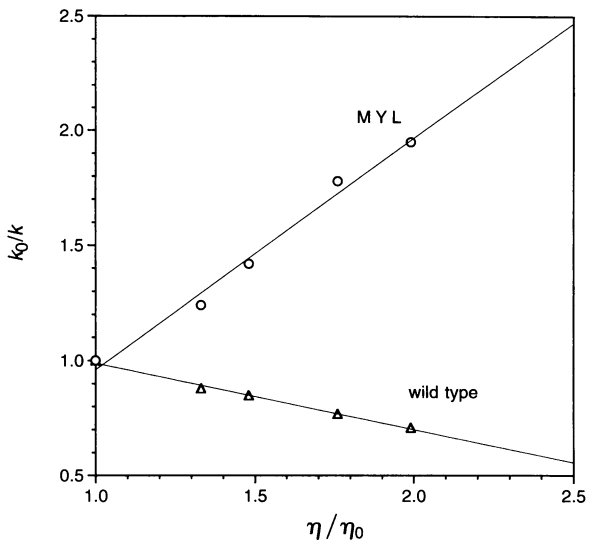

FIG. 4. Viscosity dependence of the MYL and wild-type refolding reactions (25°C, 50 mM Tris·HCl at pH 7.5/50 mM KCl/1.25 M urea/2 μM protein). The *y*-axis represents the value of the refolding rate constant determined in the absence of sucrose (k_0) divided by the value determined at each sucrose concentration. The *x*-axis is relative viscosity. The slopes of the lines are −0.29 (wild-type) and 1.01 (MYL).

transition state before any significant favorable energy was recouped by optimization of hydrogen-bond geometries. The establishment of hydrophobic interactions, by contrast, should be easier. As soon as hydrophobic groups are close enough to exclude water, there should be some favorable interaction energy even if complementary packing has not been optimized.

The refolding and unfolding of both wild-type Arc and the MYL mutant can be modeled as two-state transitions between denatured monomers and native dimers by several criteria: (*i*) equilibrium denaturation curves measured by different physical probes are superimposable with no sign of populated intermediate states; (*ii*) kinetic unfolding and refolding curves show single phases which account for the entire amplitude of each reaction; (*iii*) equilibrium constants determined experimentally are the same to within error as those calculated from kinetic constants; (*iv*) equilibrium and refolding experiments show the expected bimolecular dependence on protein concentration, while unfolding is unimolecular; and (*v*) the urea dependences of the rate constants predict the urea dependence of the equilibrium constants to within error (8, 9, 12, 13, 28). These observations indicate that any folding intermediates which do exist must be unstable relative to native dimers and denatured monomers and, thus, must be poorly populated in both equilibrium and kinetic experiments.

The differences in the refolding reactions for wild-type Arc and the MYL mutant might occur because the the folding pathways for the two proteins are completely different. As discussed below, however, the two proteins could also fold by the same basic mechanism but with a change in the rate-determining step. We favor the second model because it can explain the observed data and seems more physically reasonable. Despite the apparent two-state nature of the Arc refolding and unfolding reactions, the existence of intermediates in folding has been proposed on the basis of structural principles (9), hydrogen-exchange rates (22), and NMR studies of pressure-denatured Arc (23). The minimal model for Arc refolding with a single, dimeric intermediate is

$$2U \underset{k_{-1}}{\overset{k_1}{\rightleftharpoons}} I_2 \underset{k_{-2}}{\overset{k_2}{\rightleftharpoons}} N_2.$$

Fig. 5*C* shows reaction coordinate diagrams for this model. The first transition state (ts1) represents the encounter complex for the dimerization reaction. The second transition state (ts2) represents any high-energy structures through which the partially folded dimer must pass to form the native dimer. We propose that replacing the wild-type hydrogen bonds and salt bridges with hydrophobic interactions in the MYL mutant reduces the height of the ts2 barrier, thereby changing the step that is rate limiting for refolding. For MYL, the first kinetic barrier (ts1) would be rate limiting, and most molecules that reach the intermediate dimer would continue on to form native MYL (i.e., the free-energy folding landscape is downhill; Fig. 5*C Right*). For wild type, the second kinetic barrier (ts2) would be rate limiting, and most molecules that reach the intermediate dimer would dissociate to free monomers instead of forming native dimers (Fig. 5*C Left*). This establishes a pre-equilibrium, making the rate constant for refolding effectively equal to $k_2 \cdot k_1/k_{-1}$ or $k_2 \cdot K_1$. This ensures that the wild-type refolding reaction will be second-order in protein concentration, even though the highest free-energy barrier represents a unimolecular step. The change in the rate-limiting step from ts2 for wild type to ts1 for MYL explains why the transition state for the refolding reaction occurs earlier for MYL than for wild type.

The viscosity results can also be explained in terms of the three-state model. Increased solvent viscosity will raise the height of the ts1 dimerization barrier. For MYL, this will obviously slow refolding, as this barrier is rate limiting. For wild-type Arc, however, raising the ts1 barrier will not, by itself, affect the equilibrium populations of denatured monomer and intermediate dimer, and thus the overall rate constant for refolding ($k_2 \cdot K_1$) will remain unchanged. The small increase in the wild-type refolding rate with increasing viscosity could be explained by a small decrease in the free energy of the ts2 state. In both the wild-type and MYL models shown in Fig. 5*C*, the intermediate dimer is unstable relative to the end states and thus would never be expected to be significantly populated.

Many proteins whose folding reactions have been characterized are similar to wild-type Arc in having transition states that occur late in the folding reaction, typically with burial of 60–85% of the surface that is solvent inaccessible in the native protein (24). In this regard, the early transition state of the MYL mutant (≈40% burial of the native buried surface) is unusual. We note, however, that because this early step in MYL folding appears to represent dimerization, the slowest step in folding may simply be the time required for two MYL monomers to collide in a productive orientation. It would be interesting to test if covalently linking the two polypeptide chains in MYL would accelerate the folding reaction even more, and shift the transition state to a point later in folding.

The rate of a folding reaction will obviously be maximized if, once a protein begins to fold, it continues in a unidirectional fashion until the native structure is reached. In our model, this occurs for MYL but not for wild-type Arc. In fact, the model predicts that the majority of wild-type molecules which reach the intermediate I_2 state dissociate to denatured monomers. Similar mechanisms may also slow the folding of some monomeric proteins, by creating an uphill free-energy landscape requiring many rounds of cycling between two nonnative states before the highest free-energy barrier can be crossed. Since buried polar interactions are a relatively common feature of native proteins (25, 26), the formation of such interactions could easily create such an uphill landscape and slow folding for many different proteins. In any given case, the extent to which folding was slowed would probably depend on the extent to which the polar interactions were solvent inaccessible, the local dielectric, and the total area of polar surface buried. We note that deletion of a calcium-binding loop, containing several charged residues, from subtilisin BPN′ has been shown to

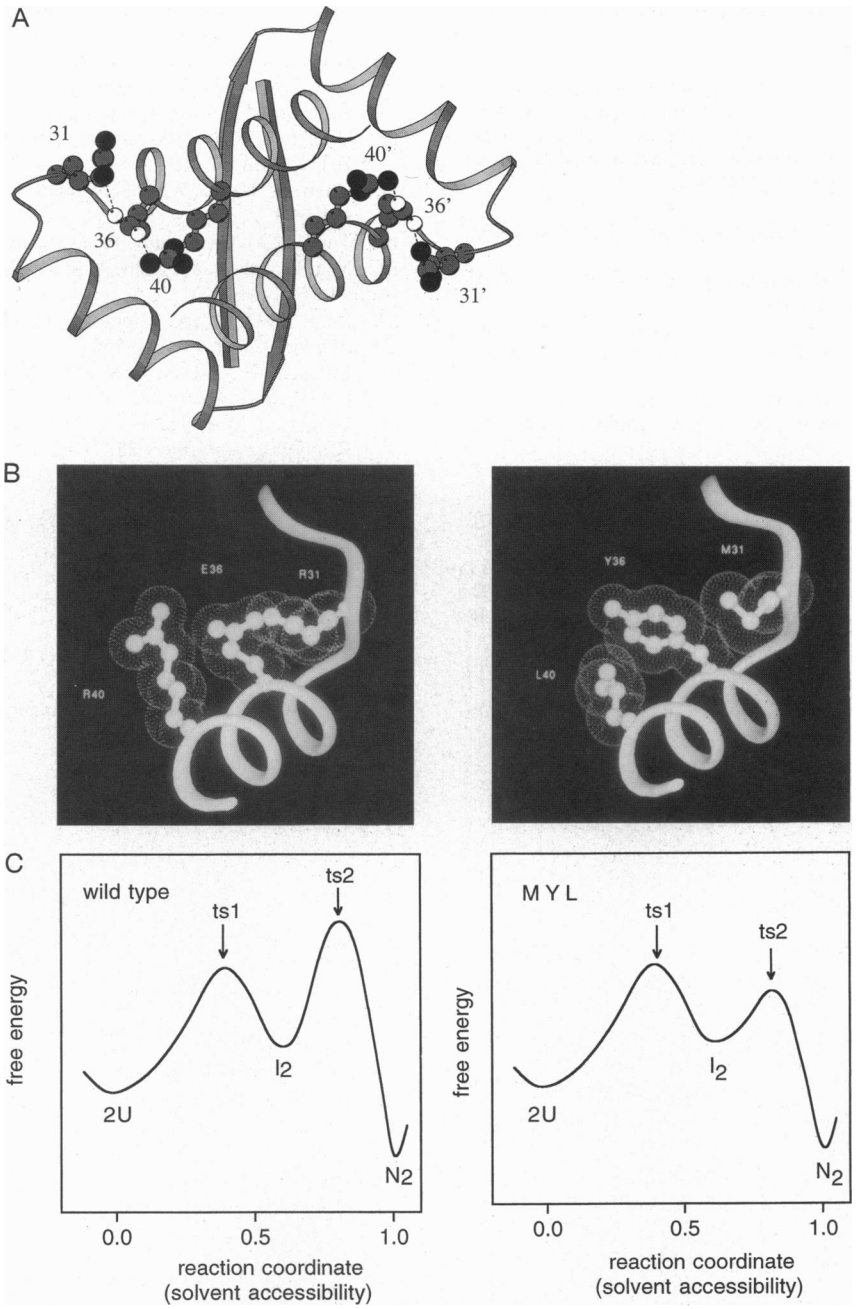

FIG. 5. (*A*) Positions of the Arg-31–Glu-36–Arg-40 salt bridges in the wild-type Arc dimer. The polypeptide backbone is shown in ribbon representation and side chains are shown in ball-and-stick representation. Hydrogen bonds are indicated by broken lines. (*B*) The wild-type side chains of Arg-31, Glu-36, and Arg-40 are shown in *Left*. The mutant side chains of Met-31, Tyr-36, and Leu-40 are shown in *Right*. Side chains are shown in ball-and-stick representation with van der Waals surfaces. Coordinates for *A* and *B* are taken from the MYL and wild-type crystal structures (ref. 12; C. Kissinger, U. Obeysekare, L. Keefe, B. Raumann, R.T.S., and C. Pabo, unpublished data). (*C*) Proposed reaction coordinate diagrams for the refolding of wild-type Arc (*Left*) and MYL (*Right*) for a model containing denatured monomers (U), a partially folded dimer (I_2), and the native dimer (N_2). The kinetic barrier between 2U and I_2 represents the dimerization reaction. This transition state (ts1) represents the encounter complex. Note that the MYL mutations are proposed to reduce the height of the ts2 barrier, making the ts1 barrier rate limiting. The free energy axis is not to scale.

increase the folding of the mutant protein to a rate that is still relatively slow (minute–hour time scale) but is significantly faster than wild type (3). We do not wish to argue that establishment of buried polar interactions is the only slow step in protein folding or that it will always be rate limiting. Dissociation of nonnative interactions may be rate limiting in some cases (27), and certain protein folds may be intrinsically difficult to assemble because of topological problems.

In the absence of urea at a protein concentration of 10 μM, the MYL mutant of Arc folds with a rate constant of 3000 s^{-1}. Several monomeric proteins, including the N-terminal domain of λ repressor (1) and the cold-shock protein CspB (2), have recently also been shown to fold in this submillisecond time regime. As a set, these proteins contain all of the structural features (tightly packed cores, α-helices, β-sheets, loops, turns, etc.) usually associated with native protein structures. As noted previously (27), it seems clear that none of the basic processes of protein folding is likely to be slow because of intrinsic physical limitations. It will be interesting to determine why some proteins require such long times to

fold and whether slow folding has any functional or evolutionary significance.

We thank Phillip Bryan, Marcos Milla, Dennis Rentzeperis, Joel Schildbach, and Frank Solomon for advice and helpful discussions. This work was supported by National Institutes of Health Grant AI-15706 and by a National Institutes of Health/National Research Service Award postdoctoral grant to C.D.W.

1. Huang, G. S. & Oas, T. G. (1995) *Proc. Natl. Acad. Sci. USA* **92,** 6878–6882.
2. Schindler, T., Herrler, M., Marahiel, M. A. & Schmid, F. X. (1995) *Nat. Struct. Biol.* **2,** 663–673.
3. Bryan, P., Alexander, P., Strausberg, S., Schwarz, F., Lan, W., Gilliland, G. & Gallagher, D. T. (1992) *Biochemistry* **31,** 4937–4945.
4. Creighton, T. E. (1986) *Methods Enzymol.* **131,** 83–106.
5. Schmid, F. X. (1993) *Annu. Rev. Biophys. Biomol. Struct.* **22,** 123–143.
6. Vershon, A. K., Youderian, P., Susskind, M. M. & Sauer, R. T. (1985) *J. Biol. Chem.* **260,** 12124–12129.
7. Breg, J. N., van Opheusden, J. H. J., Burgering, M. J., Boelens, R. & Kaptein, R. (1990) *Nature (London)* **346,** 586–589.
8. Bowie, J. U. & Sauer, R. T. (1989) *Biochemistry* **28,** 7139–7143.
9. Milla, M. E. & Sauer, R. T. (1994) *Biochemistry* **33,** 1125–1133.
10. Bonvin, A. M., Vis, H., Breg, J. N., Burgering, M. J., Boelens, R. & Kaptein, R. (1994) *J. Mol. Biol.* **236,** 328–341.
11. Raumann, B. E., Rould, M. A., Pabo, C. O. & Sauer, R. T. (1994) *Nature (London)* **367,** 754–757.
12. Waldburger, C. D., Schildbach, J. F. & Sauer, R. T. (1995) *Nat. Struct. Biol.* **2,** 122–128.
13. Milla, M. E., Brown, B. M. & Sauer, R. T. (1993) *Protein Sci.* **2,** 2198–2205.
14. Brown, B. M., Milla, M. E., Smith, T. L. & Sauer, R. T. (1994) *Nat. Struct. Biol.* **1,** 164–168.
15. Johnson, M. & Frasier, S. (1985) *Methods Enzymol.* **117,** 301–342.
16. Brenstein, R. J. (1989) NONUN (Robelko Software, Carbondale, IL), version 0.9 8b5.
17. Chen, B., Baase, W. & Schellman, J. A. (1989) *Biochemistry* **28,** 691–699.
18. Tanford, C. (1970) *Adv. Protein Chem.* **24,** 1–95.
19. Matouschek, A. & Fersht, A. R. (1993) *Proc. Natl. Acad. Sci. USA* **90,** 7814–7818.
20. Berg, O. G. & von Hippel, P. H. (1985) *Annu. Rev. Biophys. Biophys. Chem.* **14,** 131–160.
21. Milla, M. E., Brown, B. M., Waldburger, C. D. & Sauer, R. T. (1995) *Biochemistry* **34,** 13914–13919.
22. Burgering, M. J., Hald, M., Boelens, R., Breg, J. N. & Kaptein, R. (1995) *Biopolymers* **35,** 217–226.
23. Peng, X., Jonas, J. & Silva, J. L. (1993) *Proc. Natl. Acad. Sci. USA* **90,** 1776–1780.
24. Matthews, C. R. (1993) *Annu. Rev. Biochem.* **62,** 653–683.
25. Rashin, A. A. & Honig, B. (1984) *J. Mol. Biol.* **173,** 515–521.
26. Rozwarski, D. A., Gronenborn, A. M., Clore, G. M., Bazan, J. F., Bohm, A., Wlodawer, A., Hatada, M. & Karplus, P. A. (1994) *Structure* **2,** 159–173.
27. Sosnick, T. R., Mayne, L., Hiller, R. & Englander, S. W. (1994) *Nat. Struct. Biol.* **1,** 149–155.
28. Jonsson, T., Waldburger, C. & Sauer, R. T. (1996) *Biochemistry*, in press.